

# Performance Characterization of Pellet Catalytic Beds for Hydrogen Peroxide Monopropellant Rockets

A. Pasini,\* L. Torre,† L. Romeo,‡ A. Cervone,§ and L. d'Agostino¶

ALTA S.p.A., 56121 Pisa, Italy

DOI: 10.2514/1.B34000

The present paper illustrates a comprehensive experimental campaign carried out in order to assess the capability of four especially developed catalytic beds to decompose hydrogen peroxide under operational conditions representative of typical application to small monopropellant rocket engines and to characterize the resulting performance of the thruster. The catalytic beds have been integrated in a reconfigurable thruster prototype and tested in a suitable test facility. All beds have shown high decomposition and propulsive efficiencies, well in excess of 90%. In particular, two catalytic beds (indicated as LR-III-106 and CZ-11-600) have been, respectively, able to decompose up to 13 and 11 kg of 90% hydrogen peroxide (equivalent to 433 and 366 g of decomposed H<sub>2</sub>O<sub>2</sub> per gram of catalyst) in 2500 and 2000 s of continuous thruster operation. They exhibited C-star efficiencies higher than 95%. The experimental results have also indicated two main sources of catalyst degradation. In low-porosity catalysts the decay of chemical activity affects the temperature efficiency and causes the flooding of the first portion of the catalytic bed, whereas highly porous catalysts experience thermal rupture of the carrier, which leads to excessive growth of the pressure drop across the catalytic bed.

## Nomenclature

$A$	= cross-sectional area, m <sup>2</sup>
$A_t$	= throat area, m <sup>2</sup>
$c^*$	= characteristic velocity, m/s
$D$	= catalytic-bed diameter, m
$D_t$	= throat diameter, m
$F$	= thrust, N
$G$	= bed load, $\dot{m}/A$ , kg/(m <sup>2</sup> s)
$g_o$	= sea-level gravity acceleration, m/s <sup>2</sup>
$I_{sp}$	= specific impulse, s
$L$	= catalytic-bed length, m
$\dot{m}$	= propellant mass flow rate, kg/s
$p_a$	= ambient pressure, Pa
$p_c$	= chamber pressure, Pa
$R$	= gas constant of the exhaust gases, J/(kg K)
$T_{ad}$	= adiabatic decomposition temperature, K
$T_{amb}$	= ambient temperature, K
$T_c$	= combustion-chamber temperature, K
$T_{exp}$	= decomposition temperature (experimentally measured), K
$T_{1,...,5}$	= temperatures at different stations along the bed, K
$\gamma$	= specific heat ratio of the exhaust gases
$\eta_c^*$	= characteristic velocity efficiency
$\eta_{\Delta T}$	= temperature efficiency
$\tau$	= residence time, s

Paper 2009-5638 at the 45th AIAA/ASME/SAE/AIAA Joint Propulsion Conference, Denver, CO, 2–5 August 2009; received 30 April 2010; revision received 24 August 2010; accepted for publication 13 October 2010. Copyright © 2010 by the American Institute of Aeronautics and Astronautics, Inc. All rights reserved. Copies of this paper may be made for personal or internal use, on condition that the copier pay the \$10.00 per-copy fee to the Copyright Clearance Center, Inc., 222 Rosewood Drive, Danvers, MA 01923; include the code 0748-4658/11 and \$10.00 in correspondence with the CCC.

\*Project Engineer, 5 Via A. Gherardesca, Ospedaletto; Ph.D. Student, Aerospace Engineering Department, Pisa University; a.pasini@alta-space.com. Member AIAA.

†Project Manager, 5 Via A. Gherardesca, Ospedaletto; l.torre@alta-space.com. Member AIAA.

‡Project Engineer, 5 Via A. Gherardesca, Ospedaletto; Ph.D. Student, Aerospace Engineering Department, Pisa University; l.romeo@alta-space.com. Member AIAA.

§Project Manager, 5 Via A. Gherardesca, Ospedaletto; a.cervone@alta-space.com. Member AIAA.

¶Vice-President, Head of Chemical Propulsion Division; Professor, Aerospace Engineering Department, Pisa University; luca.dagostino@ing.unipi.it. Member AIAA.

## I. Introduction

THE first applications of hydrogen peroxide (H<sub>2</sub>O<sub>2</sub>) as propellant date from 1938, when it was used in the rocket-assisted takeoff system of the Heinkel He-176 aircraft and in the gas generator of the V2 rocket turbopump. Later, H<sub>2</sub>O<sub>2</sub> was used in a number of applications culminating in the attitude control system of the manned Mercury spacecraft and in the primary propulsion of the Black Arrow launcher [1]. To take advantage of the H<sub>2</sub>O<sub>2</sub> decomposition reaction in rocket propulsion applications, an effective, reliable, and durable catalytic bed is required. It should provide fast and reproducible performance, be insensitive to poisoning by stabilizers and impurities contained in the propellant [2], and be capable of sustaining the large number of thermal cycles imposed by typical mission profiles in small-satellite applications. Traditionally, pure silver and silver-coated stainless steel grids [3,4] have been the most frequent kind of H<sub>2</sub>O<sub>2</sub> catalysts in space propulsion applications, even if their use is limited to H<sub>2</sub>O<sub>2</sub> solutions with concentrations lower than 92% by weight, not to exceed the melting temperature of silver [5]. With the aim of developing more suitable substitutes, in recent years ceramic materials have been widely reconsidered for the decomposition of H<sub>2</sub>O<sub>2</sub> in gas generators or in monopropellant thrusters. In particular, both conventional alumina-based supports (extrudates, pellets, and spheres) [6,7] and honeycomb monolith carriers [8] have been used for the preparation of catalysts. Under suitable conditions, the former supports can be directly impregnated using an active phase precursor, while the latter require surface impregnation of a thin and porous washcoat layer, which is necessary to increase the relatively surface area of typical support materials, such as cordierite and mullite. The results of screening tests recently carried out by the authors, on a number of chemical species indicated platinum as the most promising catalyst for H<sub>2</sub>O<sub>2</sub> decomposition. The same tests also indicated that thermal stresses induced by the intense release of heat on the pellet surface often caused the rupture of the catalyst support into fine particles, as commonly observed by a number of investigators (Pasini et al. [9] and Sahara et al. [6]). The efforts to solve this problem recently led to the development of different Pt/α-Al<sub>2</sub>O<sub>3</sub> catalysts with a surface load of platinum close to 35% by weight and adequate thermal shock resistance (Romeo et al. [10]).

This paper illustrates the results of an experimental campaign carried out in a 6.5 N monopropellant thruster prototype on the above three Pt/α-Al<sub>2</sub>O<sub>3</sub> catalysts and on a Pt/Ce<sub>0.6</sub>Zr<sub>0.4</sub>O<sub>2</sub>/Al<sub>2</sub>O<sub>3</sub> catalyst. This catalyst consists of platinum deposited on the alumina substrate with the interposition of a ceria-zirconia film and has been prepared by means of a technique reported in Romeo et al. [11]. The

experimental campaign has been carried out under both continuous and pulsed thruster operation, in order to assess the propulsive performances of the beds and their potential degradation after the decomposition of relatively large amounts of 90% high-test peroxide. In addition, the influence of a spray injection of  $H_2O_2$  on the propulsive performance and efficiency of the thruster has also been studied.

## II. Test Apparatus

### A. Thruster Prototype

Based on the experience gained during previous experimental campaigns (Pasini et al. [9,12] and Torre et al. [13]), a new reconfigurable monopropellant thruster prototype has been designed, with special attention to substantially reducing the empty volumes and the wall thickness of the engine elements with respect to the previous prototype (Torre et al. [13]), in order to decrease as much as possible the startup transient and the wall heat losses; guaranteeing the possibility of adjusting the length of the bed and its propellant load  $G$  within reasonably wide ranges, in order to adapt them to the observed performance of the catalyst; simplifying the design and mounting of the bed housing and its related components; introducing several temperature probes along the bed in order to better detect and monitor the possible degradation of the catalytic activity; and supplying the  $H_2O_2$  to the catalytic bed by means of a suitable spray injector, in order to reduce the wetted portion of the bed (where propellant vaporization takes place, Pasini et al. [14]) as well as the thrust buildup transient.

Figure 1 shows a drawing of the cutoff assembly and a photograph of the thruster prototype used in the present experiments.

The thruster has been designed to operate with 5 g/s of 90%  $H_2O_2$  at a nominal chamber pressure of 15 bar and 10 kg/m<sup>2</sup> s of bed load (25 mm catalyst-bed diameter), developing a nominal thrust of 6.5 N. Three conical nozzles have been designed in order to change the bed load and allow atmospheric operation of the thruster without nozzle flow separation at three values of mass flow rate (5, 17, and 28 g/s) and the same chamber pressure (15 bar). Therefore the nozzles have been manufactured as separate elements, which can be easily substituted depending on the desired experimental conditions. The main element of the thruster is the cylindrical casing, which is interfaced at the fore end with the flanged connection to the thrust balance and at the aft end to the threaded nozzle. Sealing is assured by a MICATHERM S15 seal and a copper face gasket, respectively.

The catalytic reactor is provided with five temperature taps realized by means of 1/16 NPT connectors welded on the outer wall of the thruster casing. The taps are spaced axially by 10 mm starting

from the injection plate, and alternately staggered by  $\pm 60^\circ$  with respect to the vertical meridional half-plane. The maximum volume available for the catalytic bed in the channel between the injection and distribution plates is 30 cm<sup>3</sup>, with a maximum length of 60 mm. The distribution plate has a 50% open area ratio, realized by means of 210  $\times$  1.5 mm internal diameter holes for more uniform injection of the decomposition products in the combustion chamber, and a central M4 threaded hole for connection to the extraction tool. Conversely, the injection plate is an AISI304 cap-shaped grid with a 40 mesh index. Its mesh size represents a tradeoff value between the sizes of the injection droplets and of the catalyst pellets, in order to not to obstruct too much the passage of the propellant droplets through the plate and their rapid vaporization as they reach the catalyst surface.

Hydrogen peroxide injection is realized by means of a hollow-cone fine spray nozzle assembled on the adapter by means of a ring nut. The nozzle nominally operates at 5 bar of pressure drop, generating droplets with 110  $\mu m$  volumetric mean diameter and a jet angle of 58°. Once the spray injector has been mounted on its support and the catalyst has been loaded in the bed volume, the cap-shaped injection plate and its 20 N compression spring are inserted into the housing in order to retain the catalyst pellets from moving under the loads generated by the propellant flow. Finally, the exhaust nozzle is screwed in the aft part of the casing and the entire thruster is mounted by means of eight M4 bolts to the L-shaped connection with the thrust balance of test facility.

### B. Test Facility and Instrumentation

The experimental campaign has been carried out in an easily reconfigurable and expandable experimental apparatus especially designed for performance characterization of small monopropellant (e.g.,  $H_2O_2$ ) and bipropellant (e.g.,  $H_2O_2$ -hydrocarbon) [9,12,13] rocket engine prototypes and catalytic reactors operating at thrust levels in the 1–10 N and 25–100 N ranges.

The facility mainly comprises the propellant feed systems and the thrust balance. All of the hydrogen peroxide lines and main tank are made off AISI 316 stainless steel internally coated with Teflon. Hydrogen peroxide is stored in a 2.5 liter tank and is pressurized by means of nitrogen. The physical conditions of the propellant are continuously monitored by means of a J-type thermocouple and a gauge pressure transducer: if the peroxide starts to decompose, the tank can be vented to the atmosphere by means of a remotely controlled valve or, in the absence of the operator, by the combination of a relief valve and a burst disc calibrated for opening at suitably spaced pressure values. The hydrogen peroxide mass flow rate is controlled by means of interchangeable cavitating venturis and it

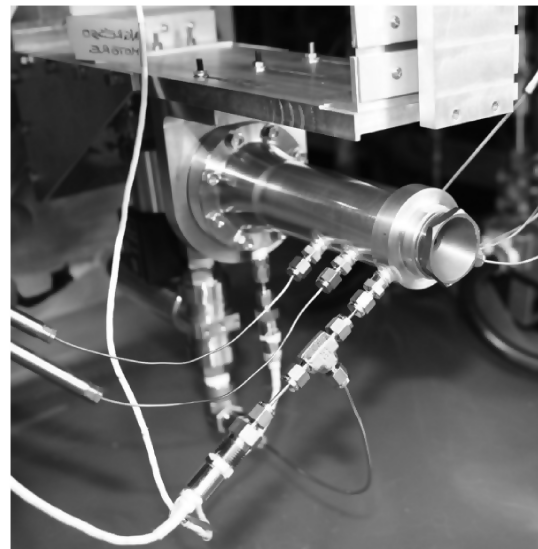
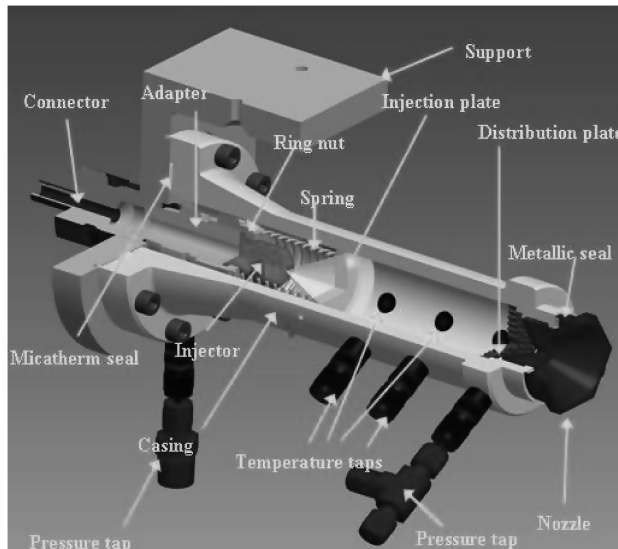


Fig. 1 Drawing of the cutoff assembly of the thruster prototype and a photograph of the thruster before a firing test.

**Table 1 Sensors list of the test facility**

Transducer	Model	Range	Accuracy	Location
Thermocouple J-type	6 mm outside diameter, mineral-insulated, by Watlow	<i>Propellant supply facility</i> −40–750°C	±1.5°C up to 375°C	Main tank
Gauge pressure transducer	PTU60 model, by Swagelok	0–60 barg	±0.43% full-scale output	Main tank
Differential pressure transducer	FP2000 model, by Honeywel	0–500 psid	±0.1% full-scale output	Across the venturi
Gauge pressure transducer	PTU40 model, by Swagelok	0–40 barg	±0.43% full-scale output	Downstream of the venturi
Coriolis mass flow meter	MFS 7100 S04 model, by Krohne	0–100 kg/h	±0.1% measured value	Downstream of the venturi
Absolute pressure transducer	XTM-190M, by Kulite	<i>Test section</i> 0–17 bara	±1% full-scale output	Downstream the injector/ combustion chamber
Differential pressure transducer	FP2000 model, by Honeywel	0–25 bard	±0.1% full-scale output	+tap: upstream of the injector; –tap: combustion chamber
Thermocouple K-type	1 mm o.d., mineral-insulated, by Tersid	−200–1350°C	±1°C up to 375°C; ±4°C at 1000°C	Along the catalytic bed/ combustion chamber
Load cell	Model 13, by Sensotec	1 kgf	±0.9% full-scale output	On the cradle

is monitored by a Coriolis flowmeter. The operation of the venturi is continuously monitored by a differential and a downstream pressure transducer.

The thruster is mounted on a one-degree-of-freedom dynamometric force balance. A number of transducers have been installed for evaluating the performance of the thruster prototype and the catalytic reactor. In particular, the conditions of the thrust chamber downstream of the catalytic bed are monitored by means of a K-type thermocouple placed on the chamber axis and by an absolute pressure transducer, which has been mounted recessed for protection from the high temperatures developing during chamber operation. A subminiature compression load cell, mounted on the balance cradle, measures the engine thrust. The performance of the catalytic bed is monitored by measuring the absolute pressure after the injector and the differential pressure between the supply line to the injector and the thrust chamber. Finally, five K-type thermocouples have been mounted along the bed for monitoring the local catalyst temperature. Table 1 reports the model, the physical range, the accuracy, and the location of all of the transducers installed in the test facility configuration used for the experimentation reported in the present paper.

A direct-current source, capable of supplying different output voltages, provides the transducers with the required electric excitations. The data coming from the sensors and transducers installed in the facility are acquired and transferred to a personal computer by means of a National Instruments acquisition board, capable of acquiring 32 analog channels and 48 digital channels at a maximum sampling rate of 1.25 megasamples per second. The acquisition board is connected to different conditioning and filtering modules, also produced by National Instruments. A LabVIEW® data acquisition and control program is used for real time display of the data and for recording all of the acquired signals. A 20 samples/s acquisition rate has been selected for compatibility with the maximum speed of the acquisition board and of the personal computer central processing unit, which represents the most stringent speed limitation of the present experimental configuration. Pressure, mass flow rate and thrust signals have been low-pass-filtered by means of a 10 Hz cutoff frequency analog Butterworth filter. A lower cutoff frequency (4 Hz) has been used for the temperature signals.

### III. Catalysts

Several catalysts have been selected for testing in the thruster prototype in the development of the present experimental campaign with the aim of assessing their chemical activity, susceptibility to poisoning, and useful life for H<sub>2</sub>O<sub>2</sub> decomposition. All of them have been prepared using 0.6 mm spheres of ceramic alumina as catalyst support. Table 2 reports the main physical and chemical properties of the tested catalysts.

Two different substrates, respectively, indicated as 0.6/4 and 0.6/75 and produced by SASOL GmbH, have been used as catalyst carriers. The 0.6/4 support consists of  $\alpha$ -Al<sub>2</sub>O<sub>3</sub> with a Brunauer–Emmett–Teller (BET) surface area of 4 m<sup>2</sup>/g, while the 0.6/75 substrate is a mixture of  $\theta$  and  $\alpha$  alumina, with a one-order-of-magnitude-higher BET surface area (75 m<sup>2</sup>/g). Three platinum catalysts, indicated as LR-III-97, LR-III-106, and LR-IV-11, have been prepared using proprietary coating techniques. Another platinum catalyst, indicated as CZ-11-600, has been prepared as reported in Romeo et al. [11]. This represents the first documented application of a Pt/Ce<sub>0.6</sub>Zr<sub>0.4</sub>O<sub>2</sub>/Al<sub>2</sub>O<sub>3</sub> catalyst to H<sub>2</sub>O<sub>2</sub> decomposition in rocket thrusters and a significant extension with respect to the traditional use of this kind of catalysts in automotive three-way converters [11].

Figure 2 shows two scanning electron micrographs of the CZ-11-600 (170 $\times$ ) and LR-III-106 (54 $\times$ ) catalysts. All catalysts have been prepared on Al<sub>2</sub>O<sub>3</sub> spheres with an average diameter of 0.6 mm. The SEM images of CZ-11-600 have been taken on a fired sample: the smaller granules have been produced during the firing tests because of substrate thermal breakup. Table 2 summarizes the main characteristics of the four catalytic systems used in the present experimental campaign. The nominal metal load indicates the percentage ratio of platinum against alumina mass. The CZ-11-600 has been specially prepared using a different nominal metal load with respect to other samples, in order to better study whether variations in catalytic activity could arise by increasing tenfold the metal content. SEM-EDX microanalyses using a standard scanning window of about 240  $\times$  200  $\mu$ m have been carried out on six different catalyst granules for all samples. For each sample the platinum load averaged over the six readings (SEM metal load) has been reported in the last column of Table 2. In consequence of different levels of penetration achieved by the precursor solution, different SEM loads have been

**Table 2 Main characteristics of the catalytic systems used in the thruster experimental campaign**

Identification code	Catalyst	Support	Nominal metal load (wt%)	SEM metal load (wt%)
LR-III-97	Pt/ $\alpha$ -Al <sub>2</sub> O <sub>3</sub>	0.6/4	2	35
LR-III-106	Pt/ $\alpha$ -Al <sub>2</sub> O <sub>3</sub>	0.6/4	1	3
LR-IV-11	Pt/ $\theta$ - $\alpha$ -Al <sub>2</sub> O <sub>3</sub>	0.6/75	1	2.5
CZ-11-600	Pt/Ce <sub>0.6</sub> Zr <sub>0.4</sub> O <sub>2</sub> /Al <sub>2</sub> O <sub>3</sub>	0.6/75	10	10

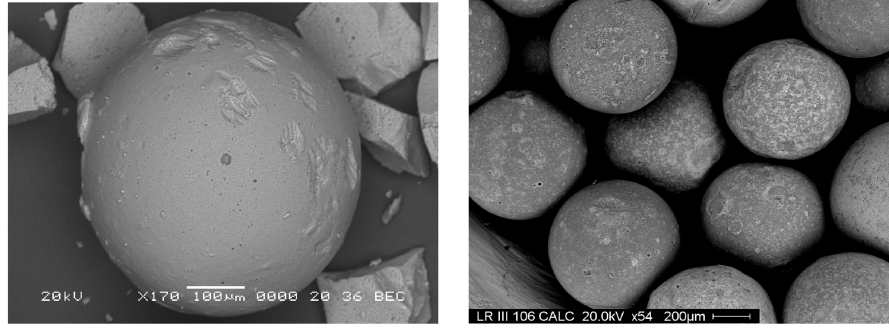


Fig. 2 SEM images of the CZ-11-600 (left) and LR-III-106 (right) catalyst samples.

observed on the catalyst samples even though the catalysts have been prepared with similar platinum contents per gram of carrier with the exception of CZ-11-600 sample.

#### IV. Experimental Results and Discussion

##### A. Catalytic-Bed Main Parameters

The characteristic velocity efficiency  $\eta_{c^*}$  and the temperature efficiency  $\eta_{\Delta T}$  have been used for quantitatively assessing the effectiveness of catalytic beds in decomposing hydrogen peroxide for thrust generation. They are, respectively, defined as

$$\eta_{c^*} = \frac{c_{\text{exp}}^*}{c_{\text{theo}}^*} = \frac{p_c^{\text{exp}} A_t}{\dot{m}_{\text{exp}}} \sqrt{\frac{RT_{\text{ad}}}{\gamma}} \left( \frac{\gamma+1}{2} \right)^{\frac{\gamma+1}{2(\gamma-1)}} \quad (1)$$

$$\eta_{\Delta T} = \frac{T_{\text{exp}} - T_{\text{amb}}}{T_{\text{ad}} - T_{\text{amb}}} \quad (2)$$

The  $c^*$  efficiency expresses the ratio between the measured characteristic velocity and the theoretical one, computed using the 1-D ideal rocket equations and the nominal adiabatic decomposition temperature  $T_{\text{ad}}$  of the propellant. Its value, lower than one, takes into account both the chemical performance of the catalyst, which can reduce the decomposition temperature below its nominal value and the nonidealities of the gas transit through the thrust chamber and the expansion nozzle. On the other hand, the temperature efficiency mainly accounts for the catalyst performance, expressing how close the measured chamber temperature is to the adiabatic temperature, corresponding to complete decomposition of the propellant.

Another important operational parameter is the pressure drop across the catalytic bed, whose magnitude adversely affects the weight of the propellant storage system. However, an excessive reduction of the bed losses reduces the fluid dynamic damping in the

bed, exposing the chamber to the risk of development of self-sustained flow oscillations. Bed losses also represent the primary source of catalyst pressurization during the engine startup. Their excessive reduction retards the pressurization of the catalyst, decreasing the propellant decomposition rate and increasing the length of the startup transient. Finally, the variation of the catalyst pressure drop gives indications about the aging of the bed and, in particular, of the occurrence of thermal fracture of the catalyst pellets.

For effective comparison between the various types of catalysts, all of the experiments have been conducted using the same concentration of hydrogen peroxide ( $90\% \pm 0.8\%$ , produced by peroxide propulsion) and the same injection nozzle at equal values of the load ( $G = 10 \text{ kg/s m}^2$ ) and length of the catalyst bed ( $L = 60 \text{ mm}$ ).

##### B. Endurance Tests on LR-III-97 and LR-III-106 Supported on Compact Alumina

The experimental campaign on the LR-III-97 has comprised four firing sessions. Figure 3 reports the time evolution of the thrust and mass flow rate as functions of cumulative time from the beginning of the test. In particular, the experimental data have been plotted only when the firing valve was open; consequently, the dead times between two firings are not reported. In the first firing (cumulative time of from 0 to 210 s), the thrust profile has been particularly smooth, due to a uniform decomposition of the hydrogen peroxide, with no significant pressure oscillations inside the thrust chamber. Both the temperature and the characteristic velocity efficiencies have been higher than 90%. The measured specific impulse for atmospheric exhaust conditions and its extrapolated value in vacuum have been slightly lower than 120 and 160 s, respectively. The initial transient of the temperature inside the bed reported in Fig. 4 shows that steady-state conditions have been reached in about 25 s and that thereafter all of the thermocouples have substantially measured the same bed temperature. The long transient has probably been the consequence of the presence of some water inside the piping line

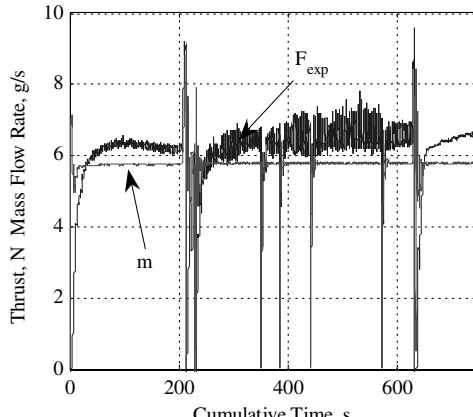


Fig. 3 Thrust and mass flow rate as functions of the cumulative time for the LR-III-97 catalyst.

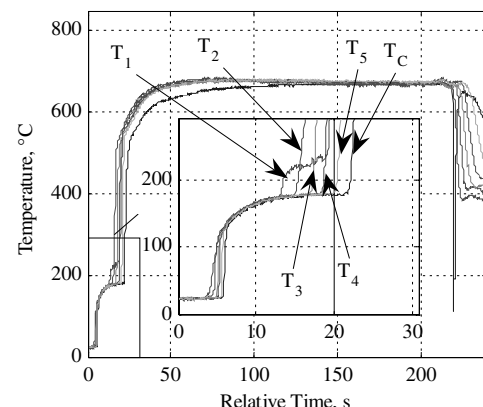


Fig. 4 Temperature profiles inside the catalytic bed in the first firing of the endurance test on LR-III-97.

from a previous purging/cleaning operations. Furthermore, Fig. 4 indicates that in steady-state conditions most of the decomposition reaction has taken place in the part of the catalytic bed upstream of the first thermocouple. The second firing has been interrupted after only 18 s because of a seal problem. In the third experiment (cumulative time of from 220 to 630 s) strong pressure oscillations have been observed, even though the mass flow rate has been kept stable near its nominal value by the cavitating venturi.

The efficiencies and the specific impulses have been almost the same for all the firings, showing good repeatability. In this case, the transient startup has been equal to about 15 s. In the final firing (cumulative time of from 630 to 740 s), the thrust has been particularly smooth, as shown in Fig. 3. The more regular profile of the thrust in the final firing with respect to the previous ones is probably related to the reestablishment of the original preload of the catalytic pellets. In particular, strong pressure and mass flow rate oscillations occurred in the third firing (Fig. 3), because the catalytic pellets had not been sufficiently packed and loaded during the assembly of the catalytic bed. Conversely, flow oscillations disappeared when the catalyst was correctly pressed, as in the last firing reported in Fig. 3.

The time evolution of the temperatures inside the catalytic bed in the last firing, reported in Fig. 5, shows the progressive degradation of the catalytic capability of the bed. In fact, the first two thermocouples have measured very low temperatures, which are symptomatic of the flooding of the first part of the bed with liquid

hydrogen peroxide. The flooding can be very dangerous in pulsed firings, as reported in Fig. 6, where the high overpressure experienced just after shutdown of the propellant valve is likely due to the rapid decomposition/vaporization of the liquid hydrogen peroxide as it flooded by gravity the much hotter and still efficient aft part of the catalytic bed.

The endurance test on the LR-III-106 catalyst has been split in five sessions. The first three sessions have been conducted according to the following duty cycle: a long initial cold firing lasting at least 120 s, followed by 40 s pulses separated by 120 s intervals. In the last two sessions, because of the partial flooding of the bed, only a single long firing of about 600 s has been carried out. During the very last session, the partially empty pressurizing vessel has not allowed for maintaining the nominal mass flow rate. In all of the experiments, the temperature and C-star efficiencies have approached unity (greater than 95%). The transient startup has been repeatable and equal to about 15 s.

Looking at the time evolution of the thrust in Fig. 7, it is possible to observe that the thrust profile of the cold firing has been stable, while the hot firings have been characterized by strong oscillations probably due to selective evaporation of hydrogen peroxide and water and the stratification of the decomposition that has led to regions where the adiabatic decomposition temperature ( $746^{\circ}\text{C}$ ) has been exceeded (see Figs. 8 and 9) and other areas where the channeling phenomenon has taken place.

The measured specific impulse for atmospheric exhaust conditions has reached the value of 120 s, corresponding to an extrapolated value of 160 s in vacuum. Only in the last two firings

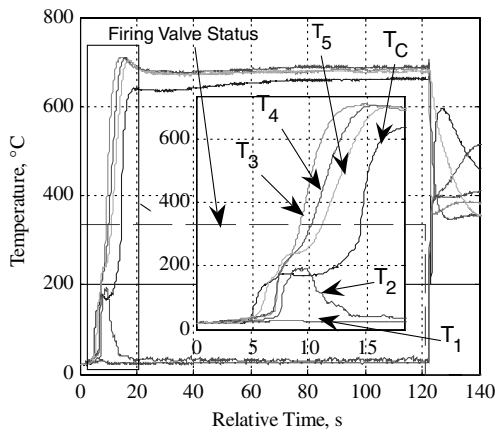


Fig. 5 Temperature profiles inside the catalytic bed in the last firing of the endurance test on LR-III-97.

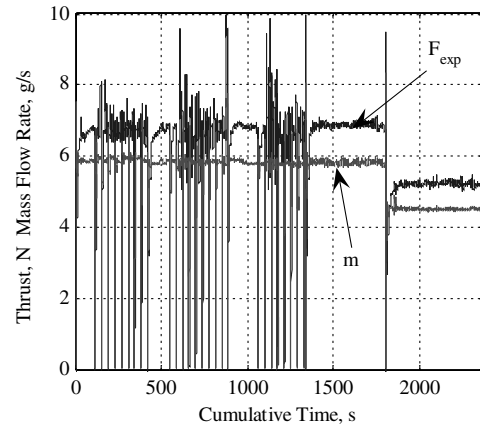


Fig. 7 Thrust and mass flow rate as a function of the cumulative time for the LR-III-106 catalyst.

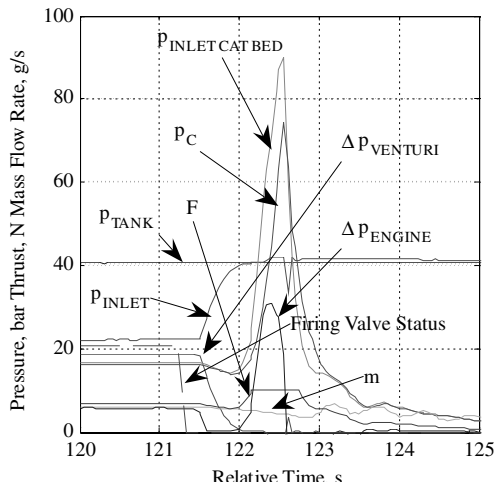


Fig. 6 High overpressure just after the shutdown of the firing valve (LR-III-97 catalyst).

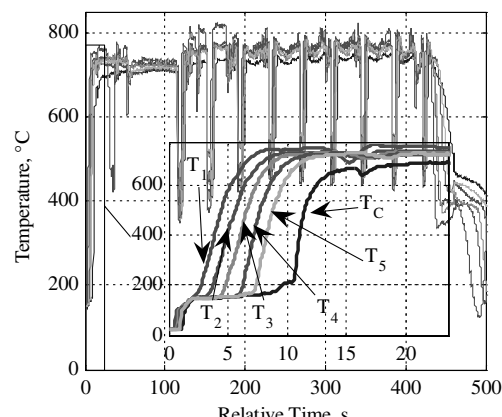


Fig. 8 Temperature profiles inside the catalytic bed in the first firing of the endurance test on LR-III-106.

first thermocouple has been intermittently flooded (see Fig. 9). The partial degradation of the first part of the bed has not produced any detectable deterioration of the propulsive performance of the thruster, because the remaining part of the bed has still been able to guarantee the complete decomposition of the hydrogen peroxide, due to the conservative values of the propellant mass flow density and residence time.

### C. Endurance Tests on LR-IV-11 and CZ-11-600 Supported on Porous Alumina

The endurance test of the LR-IV-11 catalyst has consisted of three experimental sessions with the following duty cycle: a 120 s cold-start firing, followed by 40 s pulses separated by 120 s pauses (nine pulses in the first two tests and three pulses in the last one), as shown in Fig. 10.

During the first firing (cumulative time of from 0 to 450 s) the thrust profile has displayed the occurrence of small-amplitude oscillations, probably related to the porosity of the carrier. The startup transient has lasted about 15 s, as shown in Fig. 11. The characteristic velocity efficiency has been about 95%, while the temperature efficiency has been slightly lower: 90%. During the experiment, the pressure drop across the bed has progressively increased, due to the gradual rupture of the catalyst substrate as observed after the catalyst disassembly.

In the second firing session (cumulative time of from 450 to 900 s) the performance (such as the thrust profile, the efficiencies, and the startup transient length) remained essentially unchanged. On the contrary, the pressure drop has increased almost linearly with the firing time.

The last test has been characterized by the sudden increase of the pressure drop across the catalytic bed, which led to the suppression of cavitation in the venturi and the consequent change of the propellant mass flow rate, as indicated by the data in Fig. 10.

The mass flow rate and, consequently, the thrust started to oscillate with amplitudes larger than the previous ones. Even in this case, the startup transient has been equal to about 15 s (Fig. 12), while the average propulsive performance has been consistent with previous experiments ( $\eta_c^* = 95\%$ ,  $\eta_{\Delta T} = 90\%$ , and  $I_{vsp} \cong 160$  s). The excessive pressure losses inside the bed have led to the conclusion of the endurance test, despite the absence of degradation of the catalytic activity of the bed.

The experimental data related to the endurance test on the CZ-11-600 catalyst has been reported from Figs. 13–15. In all of the five tests the thrust profile has been particularly smooth and repeatable, as shown in Fig. 13. The C-star and the temperature efficiencies have remained almost constant and equal to about 95% (see Figs. 16 and 17). Consistent with the above efficiencies, the specific impulses for atmospheric and vacuum exhaust have also reached values next to 120 and 160 s, respectively. As for the LR-IV-11 catalyst, which makes use of the same carrier, there has been a progressive increase in the pressure drop across the catalytic bed, as shown in Fig. 18. In this case the rate of degradation has been significantly lower than for the LR-IV-11 catalyst, and the life of the bed has consequently doubled (2000 s instead of 1000 s). However, the increase in the pressure drop has not affected the correct operation of the cavitating venturi, and therefore the thrust has remained essentially constant. As in the case of LR-IV-11, the occurrence of excessive pressure losses, rather than the degradation of its catalytic activity (Fig. 15), has caused the termination of the run.

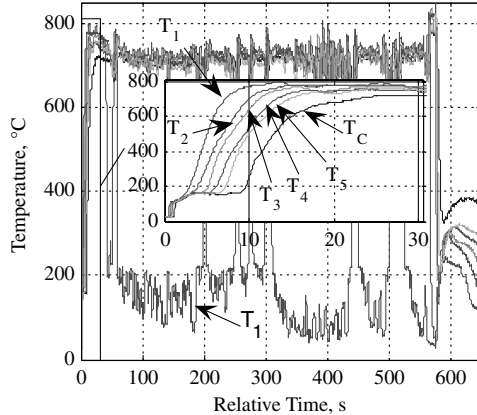


Fig. 9 Temperature profiles inside the catalytic bed in the last firing of the endurance test on LR-III-106.

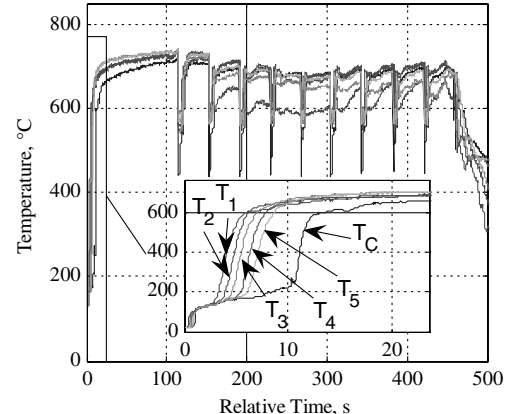


Fig. 11 Temperature profiles inside the catalytic bed in the first firing of the endurance test on LR-IV-11.

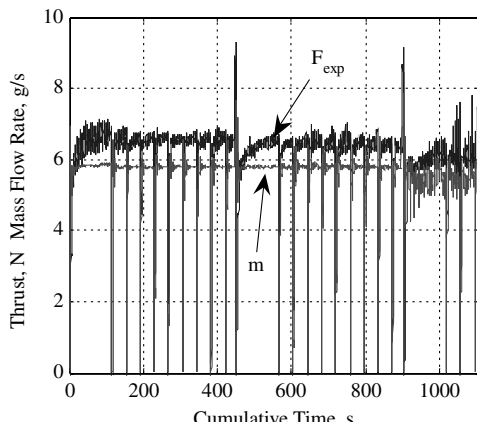


Fig. 10 Thrust and mass flow rate as a function of the cumulative time for the LR-IV-11 catalyst.

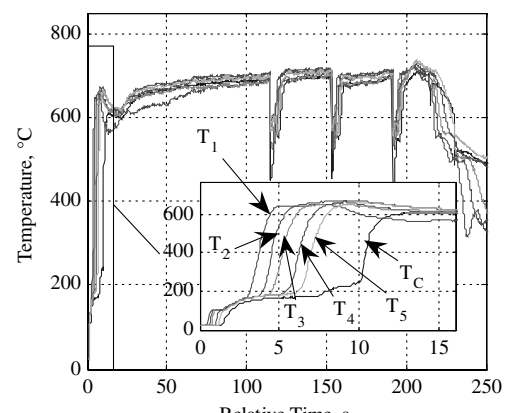


Fig. 12 Temperature profiles inside the catalytic bed in the last firing of the endurance test on LR-IV-11.

## D. Comparison Between the Performance of the Catalysts

To summarize and compare the performance and endurance of the tested catalysts it has been decided to plot in Figs. 16–18 their efficiencies and pressure drops as functions of the cumulative time from the beginning of the test. During its operational life, the C-star efficiency of the LR-III-97 has been constant, while its temperature efficiency and its bed pressure drop have slightly decreased, due to the flooding of the initial part of the bed as a consequence of the deterioration of its catalytic activity. A similar behavior has also been displayed by the LR-III-106 catalyst. Conversely, the efficiencies of both the LR-IV-11 and CZ-11-600 catalysts have remained nearly constant, while their degradation has been mostly related to the progressive and excessive raise of the bed pressure drop. In some cases the efficiencies reported in Figs. 16 and 17 exceed 100%, but they are consistent with the uncertainty range associated with the measurement errors.

In conclusion, given the properties of the catalyst carriers, Figs. 17 and 18 seem to indicate that when the substrate is thermomechanically resistant, as in the case of compact carriers, the operational life is limited by the decay of the catalytic activity, as indicated by the behavior of the temperature efficiency. On the other hand, if the carrier is relatively more porous and, consequently, less thermomechanically resistant, the catalyst life is mostly limited by the excessive raise of bed pressure drop. These are just preliminary results based on only four different catalyst types, and the previous conclusion need to be verified and confirmed by further experiments.

With reference to the thrust profiles, the analysis of the experimental data allows for the characterization of a number of critical elements for the stability and repeatability of the thrust

performance. In particular, the thrust profile is mainly influenced by the macroscopic and microscopic porosity of the bed, respectively, determined by the degree of the mechanical packing of the pellets and by the microstructure of the coating/carrier system; the uniformity of the decomposition inside the bed is strongly related to the uniformity of the deposition of the active species.

The influence of the macroscopic porosity on the stability of the thrust is manifest in the behavior of the LR-III-97 catalyst supported on compact alumina. In its first and final firings the catalyst has been correctly pressed and the thrust profile is smooth, while strong oscillations due to the insufficient packaging of the catalyst pellets appear during the third test, as shown in Fig. 3.

The effect of the microscopic porosity on the uniformity of the thrust can be observed in the comparison between the time evolutions of the thrust of the catalysts LR-IV-11 and CZ-11-600. Both of these catalysts have been realized on the same carrier, but in the CZ-11-600 sample, the ceria-zirconia film, interposed between the platinum active species and the ceramic pellets, has reduced the open porosity of the catalyst and, consequently, the intensity of the oscillations. In the catalysts supported on porous alumina, the regularity of the temperature profiles measured inside the bed have been an indirect indication of uniform decomposition. Although strong oscillations have been detected in the last firing of the LR-IV-11 catalyst (Fig. 10), these fluctuations are not associated with the porosity of the carrier, but rather with the onset of mass flow rate oscillation caused by the malfunctioning of the cavitating venturi.

Figure 7 shows that the cold firings have been smooth and repeatable, while the pulsed hot firings have been characterized by unrepeatable marked peaks. If the deposition of the catalytic element

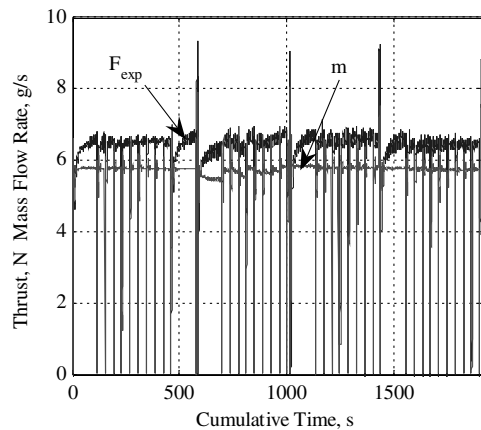


Fig. 13 Thrust and mass flow rate as a function of the cumulative time for the CZ-11-600 catalyst.

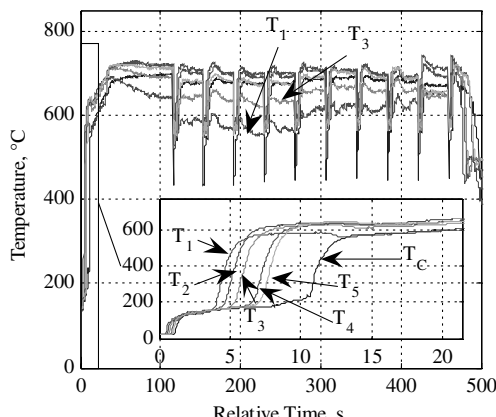


Fig. 14 Temperature profiles inside the catalytic bed in the first firing of the endurance test on CZ-11-600.

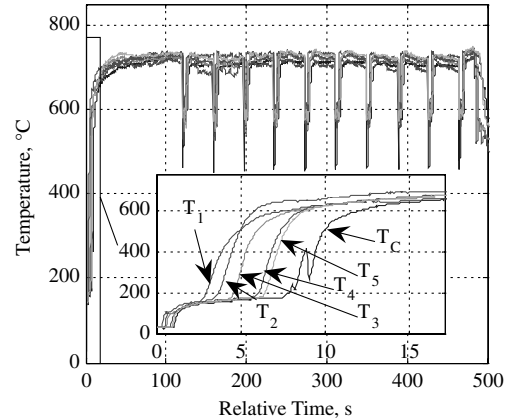


Fig. 15 Temperature profiles inside the catalytic bed in the last firing of the endurance test on CZ-11-600.

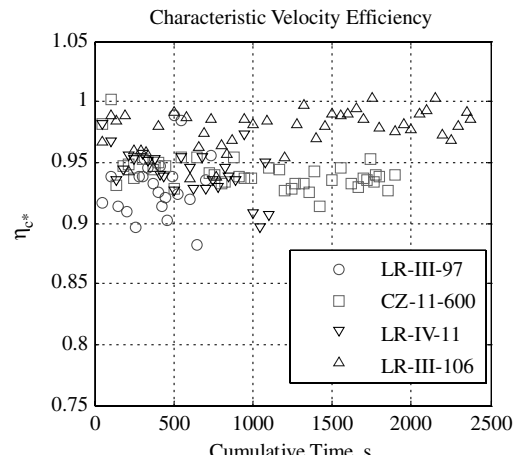


Fig. 16 Comparison between the C-star efficiency of the catalysts (maximum uncertainty in the reported measurements: 1.8%).

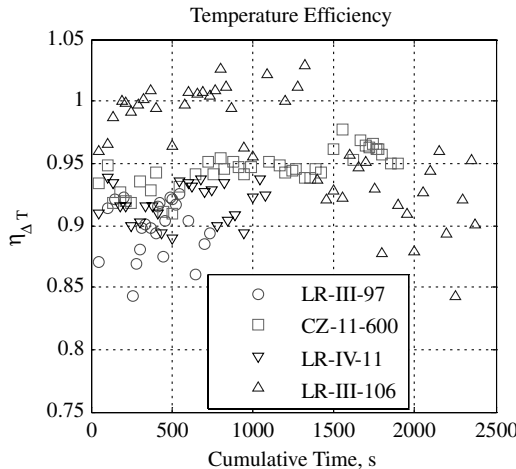


Fig. 17 Comparison between the temperature efficiency of the catalysts (maximum uncertainty in the reported measurements: 3.1%).

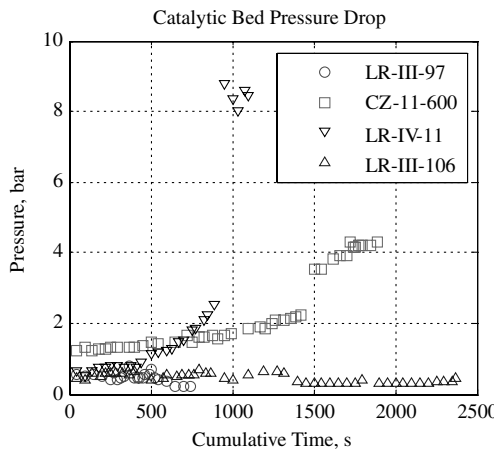


Fig. 18 Comparison between the pressure drop inside the catalytic beds.

is not uniform, as in the case of LR-III-106, the hot firings are not stable, probably because differential vaporization of water and hydrogen peroxide occurs in the already hot initial part of the bed, leading to nonuniform H<sub>2</sub>O<sub>2</sub> concentration inside the catalytic bed. As a result, regions can occur where the decomposition temperature is higher than the adiabatic decomposition temperature, corresponding to the initial hydrogen peroxide concentration. Conversely, in cold firings the hydrogen peroxide gets in touch with a cold catalyst and the vaporization of the liquid is only caused by the energy released by the catalytic decomposition, leading to a more uniform flowfield in the bed and, consequently, to smoother thrust profiles.

## V. Conclusions

An experimental campaign aimed at characterizing the propulsive performance of four different advanced catalytic beds has been carried out using an upgraded monopropellant thruster prototype equipped for measuring the decomposition temperature along the catalytic bed. The mechanical atomization of the propellant and the reduction of the empty volumes in the thruster have allowed for the significant reduction of the startup transients with respect to the previous thruster configuration (Torre et al. [13]). The current transient times (15–25 s) are still too long for typical propulsion applications and they are mainly due to the very low bed load used in the presented firings. However, realistic time responses can be attained with significantly higher mass flux in optimized designs for a given choice of the catalyst.

All of the tested catalysts showed high decomposition and propulsive efficiencies ( $\eta_{c^*} > 90\%$ ). In particular, the LR-III-106 and CZ-11-600 catalysts operated, respectively, at  $\eta_{c^*} = 98\%$  for almost 2500 s and at  $\eta_{c^*} = 95\%$  for almost 2000 s.

The experimental results have indicated two different sources of catalyst degradation. The useful life of the catalysts supported on compact carriers is limited by the reduction of catalytic activity, manifested in the decrease of the temperature efficiency and of the bed pressure drop as a consequence of the flooding of the first portion of the bed. On the other hand, the catalysts supported on highly porous substrates do not manifest appreciable degradation of the catalytic activity but suffer of the progressive rupture of the carries, which leads to excessive pressure drops across the bed.

Thrust smoothness seems to be related to the macroscopic/microscopic porosity of the bed, while the repeatability of the thrust can be associated with the uniformity of the catalyst deposition that allows for a more uniform decomposition and consequently avoids the onset of channeling.

Current work has been mostly aimed at the characterization of promising catalyst/substrate combinations under realistic conditions for operation in small rocket thrusters. Since the actual performances of the catalytic beds were not known in advance, significant margins had to be taken in the design of a flexible and reconfigurable thruster prototype. Further work will be focused on the identification of the best compromise between the various parameters (catalyst/substrate combination and preparation, pellet size, propellant injection, decomposition pressure, bed load and pressure drop, propellant dwell time, etc.) controlling the operation of catalytic hydrogen peroxide thrusters in an optimized design.

## Acknowledgments

The authors gratefully acknowledge the support of the Italian Ministry for Production Activities under D. M. 593. The authors would like to express their gratitude to Mariano Andrenucci, Fabrizio Paganucci, and Renzo Lazzaretti of the Dipartimento di Ingegneria Aerospaziale, Università di Pisa, for their constant and friendly encouragement and to the students who contributed to the project. A special thank goes to K. Shinkatsu for his continuous support.

## References

- [1] Musker, A. J., Rusek, J. J., Kappensteiner, C., and Roberts, G. T., "Hydrogen Peroxide-From Bridesmaid to Bride," *3rd International Conference on Green Propellants for Space Propulsion*, Poitiers, France, Sept. 2006.
- [2] Pirault-Roy, L., Kappensteiner, C., Guérin, M., and Eloirdi, R., "Hydrogen Peroxide Decomposition on Various Supported Catalyst Effect of Stabilizers," *Journal of Propulsion and Power*, Vol. 18, No. 6, 2002, pp. 1235–1241.  
doi:10.2514/2.6058
- [3] Runckel, J. F., Willis, C. M., and Salters, L. B., Jr., "Investigation of Catalyst Beds for 98-Percent-Concentration Hydrogen Peroxide," NASA Langley Research Center, TN D-1808, Hampton, VA, 1963.
- [4] Willis, C. M., "The Effect of Catalyst-Bed Arrangement on Thrust Buildup and Decay Time for A 90 Percent Hydrogen Peroxide Control Rocket," NASA TN D-516, 1960.
- [5] Wernimont, E., and Mullens, P., "Capabilities of Hydrogen Peroxide Catalyst Beds," AIAA Paper 2000-3555, 2000.
- [6] Sahara, H., Nakasuka, S., Sugawara, Y., and Kobayashi, C., "Demonstration of Propulsion System for Microsatellite Based on Hydrogen Peroxide in SOHLA-2 Project," AIAA Paper 2007-5575, 2007.
- [7] Romeo, L., Torre, L., Pasini, A., d'Agostino, L., and Calderazzo, F., "Development and Testing of Pt/Al<sub>2</sub>O<sub>3</sub> Catalysts for Hydrogen Peroxide Decomposition," *5th International Spacecraft Propulsion Conference and 2nd International Symposium on Propulsion for Space Transportation*, Heraklion, Crete, Greece, May 2008.
- [8] Scharlemann, C., Schiebl, M., Marhold, K., Tajmar, M., Miotti, P., Kappensteiner, C., Batonneau, Y., Brahma, R., and Hunter, C., "Development and Test of a Miniature Hydrogen Peroxide Monopropellant Thruster," AIAA Paper 2006-4550, 2006.
- [9] Pasini, A., Torre, L., Romeo, L., d'Agostino, L., Cervone, A., and Musker, A. J., "Experimental Characterization of a 5 N Hydrogen Peroxide Monopropellant Thruster Prototype," AIAA Paper 2007-

- 5464, 2007.
- [10] Romeo, L., Pasini, A., Torre, L., d'Agostino, L., and Calderazzo, F., "Comparative Characterization of Advanced Catalytic Beds for Hydrogen Peroxide Thrusters," AIAA Paper 2008-5027, 2008.
- [11] Romeo, L., Genovese, C., Torre, L., Pasini, A., Cervone, A., d'Agostino, L., Centi, G., and Perathoner, S., "Use of  $\text{Pt}/\text{Ce}_x\text{O}_2\text{-Zr}_{1-x}\text{O}_2/\text{Al}_2\text{O}_3$  as Advanced Catalyst for Hydrogen Peroxide Thrusters," AIAA Paper 2009-5637, 2009.
- [12] Pasini, A., Torre, L., Romeo, L., Cervone, A., and d'Agostino, L., "Testing and Characterization of a Hydrogen Peroxide Monopropellant Thruster," *Journal of Propulsion and Power*, Vol. 24, No. 3, May–June 2008, pp. 507–515.  
doi:10.2514/1.33121
- [13] Torre, L., Pasini, A., Romeo, L., and d'Agostino, L., "Firing Performances of Advanced Hydrogen Peroxide Catalytic Beds in a Monopropellant Thruster Prototype," AIAA Paper 2008-4937, 2008.
- [14] Pasini, A., Torre, L., Romeo, L., and d'Agostino, L., "Performance Modeling and Analysis of  $\text{H}_2\text{O}_2$  Catalytic Pellet Reactors," AIAA Paper 2008-5025, 2008.

E. Kim  
*Associate Editor*